Surface Science 287/288 (1993) 577–583
North-Holland

surface science

Surface spectroscopy from ultrathin α-Sn films on CdTe(110)

Adam Dittmar-Wituski [1] and Preben J. Møller

Department of Chemistry, H.C. Ørsted Institute, University of Copenhagen, 2100 Copenhagen, Denmark

Received 28 August 1992; accepted for publication 24 November 1992

On the basis of electron-spectroscopy results it has been deduced that α-Sn grows on CdTe(110) surfaces at coverages lower than 3 monolayers in layer-by-layer mode, followed by growth of (110)-oriented islands (Stranski–Krastanov mode). During the epitaxial growth an empty interface state due to Sn atoms appeared at 2.3 eV above the Fermi level. Band gaps in the conduction α-Sn band were found at 7.4 and 17.6 eV above the vacuum level.

1. Introduction

Tin, metastable in diamond structure (α-phase), can be grown on InSb and CdTe substrates due to nearly perfect lattice matching. The α-Sn surface has been investigated by several electron-spectroscopy techniques [1–5] but the electronic structure is not fully known. Particularly, α-Sn(110) grown on CdTe(110) has been investigated less widely as compared to the (001) surface on CdTe and InSb substrate. The CdTe(110) and CdTe(111) surfaces were reported to be less suitable as substrate than the CdTe(001) surface due to observed lower tin phase-transition temperatures [2]. To our knowledge, experimental results for determination of empty bands in this system are not available. In the present paper our aim is to investigate the electronic structure changes during growth of α-Sn on CdTe(110) by Auger, energy-loss and total-current spectroscopy, and work-function measurements (AES, EELS, TCS and WF, respectively). TCS is here applied for the first time to the Sn/CdTe system. We find that during epitaxial growth of α-Sn an empty interface state due to Sn atoms appears at 2.3 eV above the Fermi level, and that band gaps exist in the conduction α-Sn band at 7.4 and 17.6 eV above the vacuum level.

2. Experimental

Sn metal-beam-epitaxy depositions, from a Knudsen-cell evaporator, onto undoped p-CdTe(110) samples were carried out with typical quartz-crystal-calibrated evaporation rates of 0.2–0.5 Å/min (1 Å = 0.1 nm). Similar results were obtained from targets cleaved in air and targets that were spark-cut, 1/4 mm diamond-paste polished and etched in a methanol-bromine solution. Both types of samples were subsequently Ar^+-sputtered and annealed at 575 K until sharp low-energy electron diffraction (LEED) patterns at primary beam energies 50–90 eV appeared. The base pressure of 10^{-8} Pa rose to the lower 10^{-7} Pa range during the evaporation cycles. For AES and EELS a cylindrical-mirror analyzer was used. An additional separate electron gun has been built for the TCS measurements. All investigations were carried out in situ in a multi-detector chamber, described previously [6].

[1] Permanent address: Institute of Mathematics and Physics, Academy of Technology and Agriculture, Bydgoszcz, Poland.

3. Results

3.1. LEED and AES

After sputtering and annealing sharp substrate 1×1 LEED patterns have been observed. The Auger peak-to-peak signal ratio of the Cd MNN(376 eV) to Te MNN(483 eV) lines for a primary energy $E_p = 3$ keV was equal to 1.40 ± 0.05 and corresponded to an ideal stoichiometric surface [7]. No trace of TeO_2 was detected by AES. Successive evaporations of Sn caused a slightly increased background in the LEED picture until a diffuse $c(1 \times 1)$ superstructure appeared for a deposition corresponding to about 2 monolayers (ML) of α-Sn [8]. The coverage equal to 1 ML α-Sn deposited onto the CdTe(110) sample corresponds to 1.8 Å of polycrystalline Sn deposited onto the quartz crystal in the microbalance. During further Sn evaporation an increase of the background was observed, in agreement with previous observation, suggesting an amorphous growth [9]. For an overlayer thickness of ~ 10 ML an ordering was observed and (1×1) LEED patterns, with slightly increased background, indicated that the Sn layers were (110)-oriented in the α-phase. A very important requirement for the growth process was the low evaporation rate. Annealing for several minutes at temperatures not higher than 100°C during the growth process increased the quality of α-Sn layers which were found stable in ultrahigh vacuum for several weeks.

A layer-by-layer growth for the first stages of evaporation was found by AES [8]. The Auger intensity ratio $I_{Cd(MNN)}/I_{Te(MNN)}$ decreased linearly with Sn thickness during the growth of the first ML of α-Sn. At the coverage $\theta = 1$ ML a break-point was visible and the ratio of the signals then decreased with a lower rate; another change of the slope was seen at $\theta \approx 2$ ML. The analysis of the AES data indicates also a change in the ratio of the AES doublet components of the Cd and Sn lines for $0 < \theta \ll 2.5$ ML (contrary to the Te doublet). This behaviour was checked for perpendicular-incidence geometry and was reproducible. Fig. 1 shows the results from one of the experimental series.

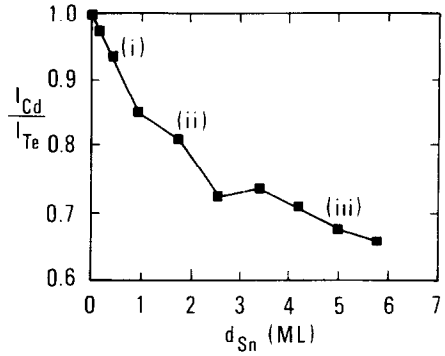

Fig. 1. Auger intensity ratio $I_{Cd(MNN)}/I_{Te(MNN)}$, normalized to the intensity $I^0_{Cd(MNN)}/I^0_{Te(MNN)}$ ($= 1.40$) for the clean substrate versus average layer thickness d_{Sn} for α-Sn deposition onto RT CdTe(110). $E_p = 3.0$ keV. The first three steps (i), (ii) and (iii) (see text) in the growth are marked.

3.2. EELS

CdTe(110) clean-substrate loss spectra were recorded for 60 eV $< E_p <$ 200 eV (table 1). Our results are in overall agreement with previous results [7,10]. The strongest surface-related losses are found at ~ 2.2, ~ 4.2 and 9.2–9.4 eV, respectively. The loss at 7.5–8.3 eV appears only for $E_p < 120$ eV. We point out that we have observed the 2.2 eV loss as a distinct one only for polished CdTe(110) samples that show a sharp 1×1 LEED picture.

The development of the EELS spectrum upon Sn deposition is shown in fig. 2 for $E_p = 200$ eV (a) and for $E_p = 75$ eV (b). For $E_p = 200$ eV the surface-sensitive losses at ~ 4.2 and ~ 9.4 eV weaken and disappear in the submonolayer region. Above 1 ML a new loss at 8.7 eV, characteristic for the Sn layer, appears. Up until $\theta = 4$ ML this loss is very pronounced (compare to the substrate losses and Sn 4d losses). Above $\theta = 6$ ML the CdTe bulk loss at ~ 10.5 eV disappears and the Sn loss at 8.7 eV shifts towards a lower energy and its intensity decreases. Subsequently, Sn deposition leads to α-Sn bulk-plasmon-loss development at 13.3 eV, and in the low-energy region losses due to interband transitions appear.

Table 1
α-Sn, β-Sn and CdTe(110) electron energy losses (eV)

Electron energy losses												
α-Sn E_p = 75 eV			α-Sn E_p = 200 eV		β-Sn/glassy carbon (200 Å film)	α + β-Sn/CdTe(110) (400 Å, fast evap.)		CdTe(110)				
0 < θ < 2 ML	Thick layer (> 40 Å)		0 < θ < 2 ML	Thick layer (> 40 Å)				E_p = 200 eV	E_p = 100 eV	E_p = 60 eV		
	2.0			2.5–3.0	3.0_w			2.9_w	2.2	2.0		
	2.5			5.1		4.2		4.3	4.2	4.1		
3.8				7.4	4.4_w			5.8	5.8	5.8		
	4.7			8.8_w	5.8_w				8.3	7.5		
5.3			8.9–8.7–7.9 [a]			6.0					$h\omega_s$	
	6.5			13.3	6.5_w			9.4	9.4	9.2		
	7.8–8.3_w	$h\omega_s$		18.8			$h\omega_s$	10.4	11.0	10.2		
8.9				21.5	10.2	9.8				12.8		
	13.3	$h\omega_p$		25.2			$h\omega_p$	14.2	13.8	13.5	Cd 4d	
	16.5		~ 26	26.1	14.0	14.0				15.8_w		
25.0				27.8		16.4		16.5	16.5	16.2	$h\omega_p$	
26.6		Sn 4d			18.8			19.5	19.8	19.5		
27.4						19.6			20.8			
					20.9				21.8	22.0		
						22.4		22.5	22.5			
					24.0							
						24.8	Sn 4d					
					25.0							
						26.2						
					27.2		$2h\omega_p$					
						28.9						
					29.0							

w: weak structures.
[a] Shift towards lower energy loss during growth process.

For $E_p = 75$ eV the surface loss at ~ 7.5 eV disappears at $\theta \approx 0.2$ ML (0.3 Å), and the 9.4 eV loss is damped, but for $\theta \approx 0.8$ ML (1.4 Å) it increases again and does not loose intensity up until $\theta = 4$ ML. Because at the same time the bulk CdTe loss at ~ 10.8 eV weakens we assume that this is the Sn-related 8.7 eV loss mentioned above. Also the intensity of the CdTe loss at ~ 2.2 eV decreases with energy, and above $\theta = 1$ ML starts to grow again. For the same reason this is a new Sn loss. The loss spectrum characteristic for α-Sn is established for $\theta \approx 11$ ML (~ 20 Å). Very remarkable is the difference between α-Sn and β-Sn losses due to the $4d_{5/2}$ and $4d_{3/2}$ excitations. For β-Sn we found these losses at 24.0 and 25.0 eV, exactly as earlier reported [11]. For $0 < \theta < 2$ ML, these losses are seen at 26.5 and 27.4 eV, however, and above $\theta \approx 1$ ML a loss appears at 25.0 eV in a step-like manner. All three losses shift gradually towards lower energies for $\theta > 10$ ML but do not reach the values of the β-Sn polycrystalline sample (the difference is about 0.8 eV).

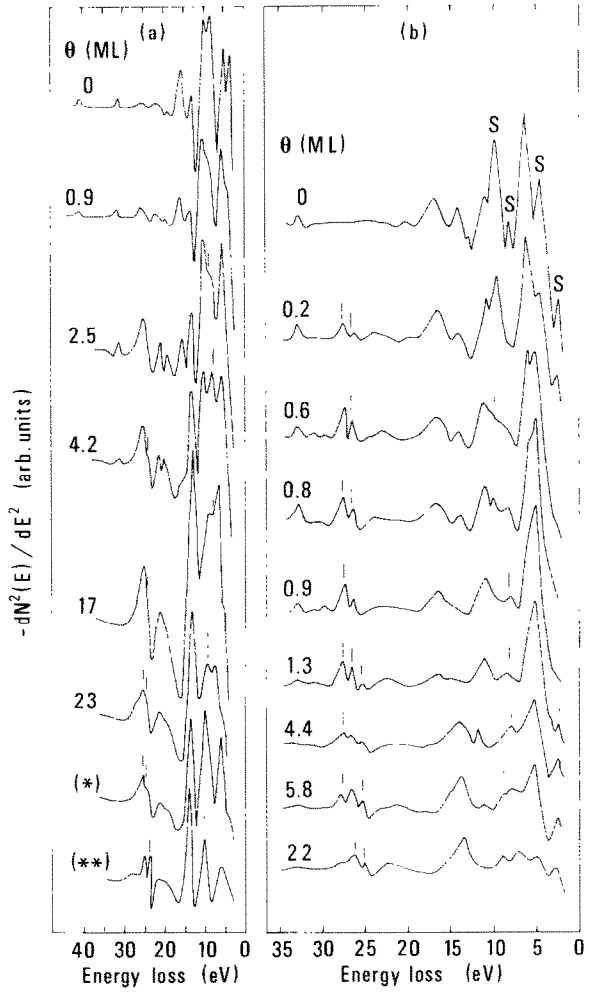

Fig. 2. Second-derivative EELS spectra during α-Sn/CdTe(110) growth at the primary energy $E_p = 200$ eV (a) and $E_p = 75$ eV (b). Panel (a): EELS spectrum from 180 Å α-Sn layer after annealing at 450 K – curve (*), and from polycrystalline β-Sn sample – curve (**). Panel (b): CdTe(110) surface losses (S), characteristic α-Sn losses (-) and α-Sn surface-plasmon loss (--).

After heat treatment above 200°C the spectra from α-Sn changed (fig. 2). For comparison, the EELS spectrum for polycrystalline β-Sn deposited in situ at the same experimental conditions on a glassy-carbon substrate is inserted in fig. 2. All energy positions of the characteristic losses from CdTe(110), α-Sn and β-Sn are presented in table 1.

3.3. TCS

TCS spectra, first derivative of the target current versus electron energy, from α-Sn at perpendicular electron-beam incidence, are presented in fig. 3. The TCS spectrum from a β-Sn sample is inserted for comparison. Due to the long mean free path of low-energy electrons in the TCS technique [12] an essential change in the TCS spectra occurs for $\theta \approx 10$ ML (20 Å), except in the low-energy region. The WF during evaporation, as measured from the contact potential difference between the sample and the cathode, decreases monotonously 0.45 eV for $0 < \theta < 2$ ML, increases again above $\theta = 3.5$ ML and finally saturates above $\theta = 8$ ML (fig. 3).

The TCS spectrum from α-Sn is dominated by two broad peaks with poorly resolved bumps. Maxima are found at 2.4 and 8.1 eV kinetic energy, respectively. A common feature of the CdTe(110) and α-Sn(110) spectra is a broad minimum which starts at ~ 15 eV kinetic energy and which, as seen for ZnO(10$\bar{1}$0) [13], corresponds to the appearance of the first LEED beams as observed by a comparative TCS experiment using LEED optics.

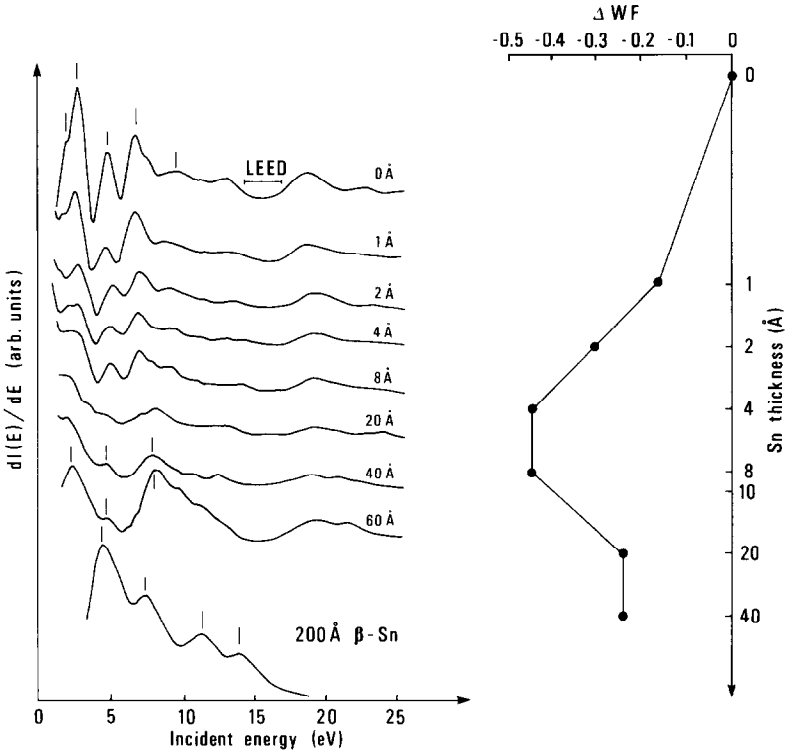

Fig. 3. TCS spectra during α-Sn/CdTe(110) growth and from a polycrystalline β-Sn sample. Characteristic structures for CdTe(110), α-Sn and β-Sn are indicated by bars. The insert shows the work-function change with coverage.

4. Discussion

For the analysis of the results presented here we first take the common features of the AES, EELS and TCS data into account. On the basis of LEED and Auger (I_{Cd} normalized to the clean surface I^{o}_{Cd} versus d_{Sn}, and I_{Sn} versus d_{Sn}) results we found [8] that Sn grows epitaxially in the Stranski–Krastanov mode (2 or 3 monolayers plus islands), rather than in the amorphous phase. From the present results we note that four steps can be distinguished during the formation of the interface and the subsequent α-Sn layer: (i) In the submonolayer range the surface losses of CdTe disappear or are significantly changed. (ii) In the layer-by-layer growth up to 3 ML the EELS spectrum shows the characteristic 8.7 eV loss as a distinct one, Sn 4d losses are shifted, and at $\theta \approx 2$ ML the Sn $4d_{5/2}$ loss appears at 25.0 eV. From the TCS data we observe a decrease in WF towards the minimum above $\theta = 2$ ML and from AES a change of the Cd and Sn line shape for $0 < \theta < 2.5$ ML. All these observations indicate a change in the electron structure and bonding character for Sn coverages above 2.5 ML. (iii) During the growth of (110)-oriented islands, above $\theta = 4$ ML, the WF increases (0.25 eV) and the LEED picture disappears because of the increase of the diffuse background. (iv) For high coverages, above $\theta \approx 10$ ML, a uniform α-Sn layer is formed. The number of defects has probably increased substantially now, since the α-Sn LEED picture is slightly less sharp than for the CdTe(110) substrate.

The change of the I_{Cd}/I_{Te} ratio for $\theta < 1$ ML suggests a faster decrease of the I_{Cd} signal than of the I_{Te} signal. This could be explained, however, by the longer escape depth of the 483 eV Te electrons comparing to 376 eV Cd electrons (the averaged escape depths at these energies calculated from the exponential decay best fit to our AES data for 4 ML $< \theta <$ 10 ML were found to

be $\lambda_{Cd} = 3.8$ ML and $\lambda_{Te} = 5.7$ ML, respectively), but for 1 ML the ratio I_{Cd}/I_{Te} measured from experiment is 10% lower than expected due to the difference in escape depths. Also the modelling, assuming layer-by-layer growth in the first stages of growth, would require a slower decrease of I_{Cd}/I_{Te} to fit the measured θ-dependence than expected from the difference in escape depths. The stoichiometric (110) surface of CdTe contains an equal number of Cd and Te atoms, and spectroscopically the two outer layers of CdTe are visible by the Auger spectrometer. The facts mentioned above, as well as LEED investigations [8], suggest that Sn atoms preferably adsorb on Cd sites of the first and second layers of the CdTe substrate. Sn atoms then adsorb not exactly in accordance with the ideal bulk diamond structure. For the mass coverage $\theta = 1$ ML, two Sn atoms must adsorb in one surface unit cell, giving rise to a centred superstructure with a bond length different from that of bulk α-Sn [8].

The substrate–overlayer interaction is also reflected in the Sn 4d core-level spin–orbit split doublet. One may argue that the ~ 27 eV loss is simply a double ~ 13 eV substrate loss, but from comparison of intensities it is definitely not the case. At $E_p \approx 70$ eV, the intensity of the 27.4 eV loss for $\theta = 0.5$ ML (≈ 1 Å) Sn is larger than the 13.6 Cd 4d substrate loss. The structures in the d-region (fig. 2) probably reflect two phases of the overlayer – one just at the interface and one due to tetrahedral α-Sn bond formation. The binding energies of the Sn 4d core levels for an 8 ML α-Sn(110) layer were reported at 25.1 and 24.0 eV with reference to the Fermi level (E_F) and were shifted 0.15 eV towards higher energies as compared to a β-Sn metallic film [14]. If we assume the same binding energy for coverages $\theta \approx 1$ ML we find an identical final-level position for both spin–orbit-split 4d-levels: $-25.1 + 27.4 = -24.0 + 26.3 = 2.3$ above E_F. One possible explanation of the observed features may be excitation of electrons to an interface empty state located 2.3 eV above E_F. In the TCS data we observe a shift of the whole spectrum relative ot the retarding voltage with increasing Sn thickness until $\theta = 2$ ML, which means that the WF change is caused by the E_F shift towards the conduction band [12c]. Because the Sn 4d losses start to shift towards lower energies for $\theta > 10$ ML, the final-level position is independent of E_F movement. Hence, this local level is pinned to the Sn-atom side of the interface which is expected to be abrupt [14].

It is perhaps surprising that in EELS we do not see the intensive surface-plasmon loss for α-Sn(110) which is the most pronounced one for the β-Sn sample at ~ 10 eV (fig. 2). After annealing above 450 K the EELS spectrum of α-Sn changed to the spectrum characteristic for β-Sn, i.e. the bulk plasmon shifted towards higher energies and the surface-plasmon peak developed, but this change outstripped the disappearance of (110) long-range order in the diffraction pattern. This fact is consistent with previous results [2] which indicate initial growth of β-Sn crystallites at structural imperfections, i.e., two phases coexist and the phase transition extends in time. We cannot make a definite statement about the temperature of the phase transition on the basis of our EELS and LEED results, however. Only for α-Sn layers of $\theta < 15$ ML the phase-transition temperature was well above 400 K; higher than reported elsewhere. For such a thin layer, immediately after the change of the loss spectra occurred, appearance of the substrate AES signal indicated islanding, and tin was removed from the substrate surface due to CdTe sublimation which is efficient above 500 K. The plasmon loss during the phase transition develops from the broad 8.7 eV loss of α-Sn. We suggest assignment of the loss at 8.7 eV to a surface plasmon of α-Sn. Both the low intensity and the observation that the value is lower than expected from the free-electron model [8] can be explained by the islanding.

The CdTe(110) surface was investigated previously by TCS [15,16] and the results were interpreted on the basis of the inelastic model [12]. To distinguish the elastic reflection from empty bands due to wave-function matching from inelastic structures in the TCS data, our TCS spectra were integrated numerically, the decreasing background which is due to secondary electron emission was subtracted and subsequently all the spectra from fig. 3 were normalized to the elastic

Bragg-reflection trough, extending above 15 eV kinetic energy. After this procedure all weak structures are smeared out and the spectra from α-Sn (semi-metal) overlayer should reflect elastic electron reflection from gaps in the conduction band, because inelastic excitations are not pronounced in the target current for metals [17]. The minimum in the target current, which corresponds to the band gap, extends for both CdTe and α-Sn from 16 to 20 eV above the vacuum level (E_v) and is centred at 17.6 eV above E_v. For the comparative β-Sn sample a minimum is also visible, but that is two times broader and shifted towards ~ 18.7 eV. In the low-energy region another minimum shifts from 5.2 eV for CdTe(110) to 7.4 eV for α-Sn. For β-Sn in the similarly integrated spectrum there is a broad maximum. We conclude that band gaps exist at 7.4 and 17.6 eV above E_v in the α-Sn conduction band.

Planned further investigations using synchrotron-radiation based angle-resolved measurements are expected to elucidate in more detail the band structure of this system which is at present of interest, due to the status of CdTe(110) as one of the cleavage-surface tetrahedrally coordinated compound-semiconductor electronic materials.

Acknowledgements

The work was supported in part by the Danish–Polish Cultural Agreement Programme and the Danish Center for Surface Reactivity. A.D.-W. acknowledges partial support by the Polish Committee of Scientific Investigations, grant No. 2 2359 9102. We are grateful to U. Blinowska from the Institute of Physics of the Polish Academy of Sciences for kindly providing the sample.

References

[1] R.F. Farrow, D.S. Robertson, G.M. Williams, A.G. Cullis, G.R. Jones, I.M. Young and P.N.J. Dennis, J. Cryst. Growth 54 (1981) 507.
[2] J.L. Reno and L.L. Stephenson, Appl. Phys. Lett. 54 (1989) 2207.
[3] H. Höchst and I. Hernández-Calderón, Surf. Sci. 126 (1983) 25.
[4] R.C. Bowman, Jr., P.M. Adams, M.A. Engelhardt and H. Höchst, J. Vac. Sci. Technol. A 8 (1990) 1577.
[5] S. Takatani and Y.W. Chung, Phys. Rev. 31 (1985) 2290.
[6] P.J. Møller and J.W. He, Nucl. Instrum. Methods B 17 (1986) 137.
[7] A. Ebina, K. Asano and T. Takahashi, Phys. Rev. B 22 (1980) 1980.
[8] P.J. Møller and A. Dittmar-Wituski, Mater. Sci. Eng. B (1992), in press.
[9] M. Mattern and H. Lüth, Surf. Sci. 126 (1983) 502.
[10] R.L. Hengehold and F.L. Pedrotti, Phys. Rev. 6 (1972) 2262.
[11] A.J. Bevolo, J.D. Verhoeven and M. Noack, Surf. Sci. 134 (1983) 499.
[12] (a) S.A. Komolov and L.T. Chadderton, Surf. Sci. 90 (1979) 359;
(b) P.J. Møller and M.H. Mohamed, Vacuum 35 (1985) 29;
(c) S.A. Komolov, Total Current Spectroscopy of Surfaces (Gordon and Breach, Philadelphia, PA, 1992).
[13] P.J. Møller and S.A. Komolov, in: Proc. Joint Nordic Spring Meeting '92, Nyborg (Risø R-628) Ed. P.A. Lindgård (1992) p. 79.
[14] H. Höchst, D.W. Niles and I. Hernández-Calderón, J. Vac. Sci. Technol. B 6 (1988) 1219.
[15] S.A. Komolov and A.F. Pigulevskii, Phys. Chem. Mech. Surf. 1 (1982) 922.
[16] M. Naparty, A. Dittmar-Wituski and J. Skonieczny, Surf. Sci. 200 (1988) 519.
[17] R.C. Jaklevic and L.C. Davis, Phys. Rev. B 26 (1982) 5391.